# Statistical Description of SaO$_2$–SpO$_2$ Relationship for Model of Oxygenation in Premature Infants

**Veronika Rafl-Huttova** [1,*], **Jakub Rafl** [1], **Knut Möller** [2], **Thomas E. Bachman** [1], **Petr Kudrna** [1] **and Martin Rozanek** [1]

1. Department of Biomedical Technology, Faculty of Biomedical Engineering, Czech Technical University in Prague, 27201 Kladno, Czech Republic; rafl@fbmi.cvut.cz (J.R.); tbachman@me.com (T.E.B.); petr.kudrna@fbmi.cvut.cz (P.K.); rozanek@fbmi.cvut.cz (M.R.)
2. Institute of Technical Medicine, Furtwangen University, 78054 Villingen-Schwenningen, Germany; moe@hs-furtwangen.de
* Correspondence: veronika.huttova@fbmi.cvut.cz

**Abstract:** A pulse oximeter model linking arterial (SaO$_2$) and peripheral (SpO$_2$) oxygen saturation is the terminal part of a mathematical model of neonatal oxygen transport. Previous studies have confirmed the overestimation of oxygen saturation measured by pulse oximetry in neonates compared to arterial oxygen saturation and the large variability of measured values over time caused by measurement inaccuracies. This work aimed to determine the SpO$_2$ measurement noise that affects the biased SpO$_2$ value at each time point and integrate the noise description with the systematic bias between SaO$_2$ and SpO$_2$. The SaO$_2$–SpO$_2$ bias was based on previously published clinical data from pathological patients younger than 60 days requiring ventilatory support. The statistical properties of the random SpO$_2$ measurement noise were estimated from the SpO$_2$ continuous recordings of 21 pathological and 21 physiological neonates. The result of the work is a comprehensive characterization of the properties of a pulse oximeter model describing the transfer of the input SaO$_2$ value to the output SpO$_2$ value, including the bias and noise typical for the bedside monitoring of neonates. These results will help to improve a computer model of neonatal oxygen transport.

**Keywords:** SaO$_2$–SpO$_2$ bias; SpO$_2$ measurement noise; noise model; neonatal model; oxygenation; pulse oximetry; oxygen saturation

## 1. Introduction

The advantages of closed-loop control of oxygenation in neonates compared to manual control have been documented in recently published clinical trials. During automatic control, arterial blood oxygen saturation remains within the desired safe range for significantly longer periods [1–6]. In the last ten years, many articles have introduced closed-loop control algorithms of oxygenation in neonates, but a complex clinical study to compare the effectiveness of those various algorithms is still missing [6]. Clinical tests of the new oxygenation control algorithms of neonates bring safety and ethical risks, but a mathematical model of oxygenation in neonates can allow for the in silico simulation of oxygenation and preliminary comparison of the control algorithms [7–10].

A general scheme of a complex mathematical model of automatic oxygenation of a neonate is shown in Figure 1. The terminal part of the model is the pulse oximeter module. In the absence of arterial blood gas measurement, both the automatic and manual control of oxygenation usually depend on pulse oximetry [1,7,11]. Many studies showed inaccuracies in the pulse oximetry measurement in children and premature infants. Peripheral oxygen saturation measured by pulse oximetry (SpO$_2$) typically overestimates arterial oxygen saturation (SaO$_2$), especially at the lower values of SaO$_2$ that are common in critically ill premature infants and children. Bohnhorst et al. noted the presence of the SaO$_2$–SpO$_2$ bias in Reference [12], where the authors determined the sensitivity

and specificity of different pulse oximeters in the detection of hyperoxemia in 56 infants. Gerstmann et al. [13] found that $SpO_2$ generally overestimated $SaO_2$ at low levels and that the spread in the data increased with lower $SaO_2$. The results were confirmed a few years later by Rosychuk et al. [14] in neonates with an average weight of 1 kg. The authors used a new generation of pulse oximeters with lower susceptibility to motion artifacts. Harris et al. [15] evaluated two sensors with improved accuracy in children with $SaO_2$ less than 85%. This study revealed statistically significant increasing bias and variability of $SpO_2$ for decreasing levels of $SaO_2$ and the authors concluded that pulse oximetry alone should not be relied upon for clinical decision-making when saturation is below 85%. In another study, Harris et al. [16] confirmed their previous findings and set the average bias at 4.0% and 7.4%, respectively, depending on the type of pulse oximeter. A similar average bias of 5.4% across all saturation levels was found by Murphy et al. [17] in a study of 89 patients with critical congenital heart disease. Ross et al. [11] described a significant variation in the $SpO_2$ accuracy. The authors computed the $SaO_2$–$SpO_2$ bias (0.2–6.6%) and precision (3.4–6.6%), expressed as the standard deviation, for seven intervals in the range of 65–97% $SpO_2$ in 225 mechanically ventilated children with cyanotic congenital heart disease or acute hypoxemic respiratory failure. Very similar results were provided in the study of Bachman et al. [18] by evaluating 25 032 $SaO_2$–$SpO_2$ measurements from 1007 critically ill neonates, or in the study of Griksaitis et al. [19] in 25 children with cyanotic congenital heart disease.
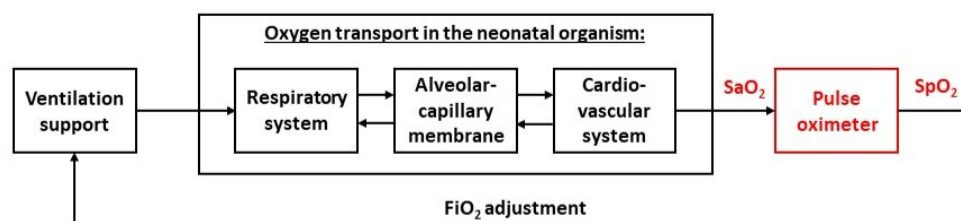
**Figure 1.** A general concept of the mathematical model of neonatal oxygen transport. The pulse oximeter module, with arterial oxygen saturation ($SaO_2$) as the input and peripheral oxygen saturation ($SpO_2$) as the output, is the terminal part of the global model.

Several studies [11,13–15,18] pointed out not only the bias between $SaO_2$ and $SpO_2$ ($SaO_2$–$SpO_2$ bias) but also quite a large variability in the bias. This variability can be caused by many factors that affect the accuracy of the pulse oximeter measurement. In the multicenter study [11], the variability in the bias could have been caused by institutional variation, for example, by using pulse oximeters from different manufacturers. A location of probe placement can influence measured $SpO_2$ values [11,20,21]; however, Harris et al. [15] did not show a significant difference between standard and nonstandard probe location. The studies [11,18] involved premature infants who could have had increased levels of fetal hemoglobin (HbF) that may alter the $SaO_2$–$SpO_2$ bias [11,14,20,22]. In addition to HbF, other hemoglobin derivates, such as carboxyhemoglobin or methemoglobin, may also affect the accuracy of the measurement [21,22].

Besides the interpersonal variability, experimental data also contain intrapersonal variability in time. A low pulsatile signal (low perfusion), high noise (bright light, electromagnetic interference, or motion), or a combination of these factors can cause a low signal-to-noise ratio, leading to inaccurate pulse oximeter readings [21,23,24]. Even when $SaO_2$ remains practically unchanged, the $SpO_2$ values presented by the pulse oximeter change in time, and in the case of abrupt motion of a neonate, they may even be falsely interpreted as rapid desaturations [23].

Recent studies dealing with noise and its filtering in relation to pulse oximetry focused on the photoplethysmography curve used by pulse oximeters. Fine et al. [25] summarized several ways of detecting noise or motion artifacts, which included using the low-signal-quality index, filters with cross-correlation, analyzing the morphology of the signal, or higher-order statistics in both the frequency and time domain. Lee et al. [26] proposed

a motion artifact reduction algorithm, using independent component analysis. Other studies [27,28] assessed the quality of $SaO_2$ estimation from photoplethysmography and detected poor-quality segments by methods of machine learning. However, the considered global model of neonatal oxygenation [8] does not consider the pulsatility in the cardio-vascular system and, thus, the photoplethysmography curve. Instead, the pulse oximeter module is treated as a black box that converts a continuous $SaO_2$ signal to a stream of trend $SpO_2$ values, reported every 2 s, that is used by automatic closed-loop control algorithms to adjust the fraction of inspired oxygen in the model input. A pulse oximeter model transforming $SaO_2$ to the observed $SpO_2$ value was used by Morozoff et al. [29]. The model adds two types of noise to the $SaO_2$ signal: the sensor noise modeled as the white noise and motion artifacts produced by a pulse generator. However, this approach is not based on real data from clinical practice.

The aim of this work was to statistically describe the $SpO_2$ measurement noise characteristic of continuous time recording of $SpO_2$ based on the evaluation of available clinical data and to combine the noise description with the systematic bias between $SaO_2$ and $SpO_2$ into a plausible mathematical model of the pulse oximeter output signal. The results of the work were intended for integration into an overall computer model of premature infant oxygenation.

## 2. Materials and Methods

The input of the pulse oximeter module of the overall oxygenation model is the continuous $SaO_2$ signal. The output signal of the pulse oximeter module consists of two principal components: the $SaO_2$–$SpO_2$ bias and the $SpO_2$ measurement noise. The $SaO_2$–$SpO_2$ bias describes a typical deviation of the $SpO_2$ measurement as a function of $SaO_2$ value. The $SpO_2$ measurement noise is a random process that changes the biased $SpO_2$ value at each time point. Data for both the components of the pulse oximeter model were processed in Matlab R2021a (MathWorks, Natick, MA, USA).

### 2.1. SaO₂–SpO₂ Bias

The $SaO_2$–$SpO_2$ bias function was determined in our previous study [30] based on clinical data acquired by Ross et al. [11]. We used the part of the data that included mechanically ventilated hypoxemic premature and term infants aged between the 37th week of gestation and the 60th day after delivery. We evaluated 1423 $SaO_2$–$SpO_2$ data pairs. The $SaO_2$ values were measured by CO-oximetry, and the $SpO_2$ values were measured by Masimo or Nellcor pulse oximeters at the same time the arterial blood sample was taken. We calculated the bias in three neighboring intervals. For $SaO_2$ below 70%, the $SpO_2$ bias was kept constant and equal to the 7.66%, which was the $SpO_2$ bias at $SaO_2$ = 70%. For $SaO_2$ in the range of 70–96%, the median of measured $SpO_2$ values was calculated for each unit value of $SaO_2$ and a third-order polynomial was fitted through the medians. For $SaO_2$ above 96%, the bias was set as zero, that is, $SpO_2$ = $SaO_2$. The $SaO_2$–$SpO_2$ bias function is displayed in Figure 2 and mathematically expressed by the following equations:
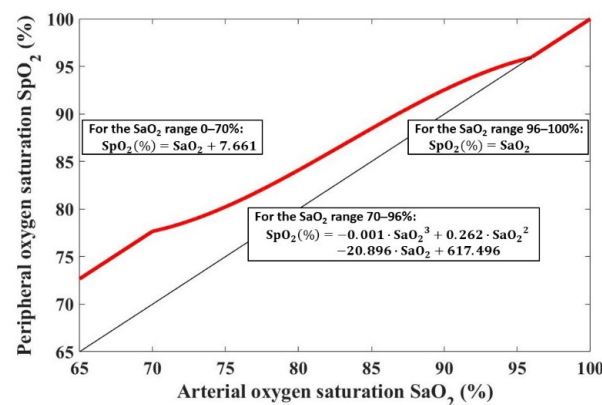
**Figure 2.** The $SaO_2$–$SpO_2$ bias function is shown with a red line. The black line shows $SpO_2$ = $SaO_2$.

- For the SaO$_2$ range 0–70%:

$$\text{SpO}_2(\%) = \text{SaO}_2 + \text{SpO}_2^{(\text{SaO}_2=70\%)} = \text{SaO}_2 + 7.66$$

- For the SaO$_2$ range 70–96%:

$$\text{SpO}_2(\%) = -0.001 \cdot \text{SaO}_2{}^3 + 0.262 \cdot \text{SaO}_2{}^2 - 20.896 \cdot \text{SaO}_2 + 617.496$$

- For the SaO$_2$ range 96–100%:

$$\text{SpO}_2(\%) = \text{SaO}_2$$

*2.2. SpO$_2$ Measurement Noise*

We based the model of SpO$_2$ measurement noise on continuous neonatal SpO$_2$ recordings from the General University Hospital in Prague. The data were collected during routine clinical care, based on a standard informed consent to hospitalization and to collection of anonymous observational data for research and educational purposes that was signed by a legal representative of a neonate. Anonymized observational data were provided to the authors of this study.

In total, we evaluated SpO$_2$ recordings from 42 patients divided into two categories: physiological neonates and pathological neonates. Twenty-one healthy physiological patients were term infants without any known pathology who were measured during the first hours after delivery. The recording time for each physiological patient was 3–21 h. Twenty-one pathological patients were premature (born before 28th week of gestation), with various diagnosed pathologies requiring oxygen support, most commonly bronchopulmonary dysplasia. The recording time for each pathological patient was 10–95 h. SpO$_2$ values were measured by Masimo Rad-97 pulse oximeter (Masimo Corporation, Irvine, CA, USA), with the sampling time set to 2 s and the averaging time set to 8 s.

2.2.1. Data Processing

The SpO$_2$ measurement noise was considered as a random process that affects the biased SpO$_2$ values at each time point. A noise-free SpO$_2$ value (SpO$_2^{\text{clear}}$) was estimated for each measured SpO$_2$ value (SpO$_2^{\text{meas}}$), and the difference of these parameters was considered as the noise component. The procedure of the noise estimation is shown in the flowchart in Figure 3 and is described in detail below.

Step 1: The unstable parts of the measured SpO$_2$ signal (SpO$_2^{\text{meas}}$), which were defined based on the study by Wellington et al. [31], were excluded from further processing. All SpO$_2$ values that met at least one of the following two criteria were excluded: (1) The SpO$_2$ value was measured at the time when the low-signal-quality alarm was triggered. The low-signal-quality alarm is a pulse oximeter indicator of potentially erroneous data; however, it does not guarantee the perfect quality of all other parts of the SpO$_2$ signal. (2) The SpO$_2$ value was the middle sample of a 30 s moving window in which SpO$_2$ changed by more than 10%. An example of the original raw SpO$_2^{\text{meas}}$ signal with identified stable and unstable parts is shown in Figure 4. Step 2: All null or unavailable data points in the SpO$_2^{\text{meas}}$ signal were replaced by the nearest preceding valid SpO$_2$ value. The replaced values were not included in calculations of the SpO$_2$ measurement noise. The aim of replacing the null and unavailable values was to avoid abrupt transitions to zero values in SpO$_2^{\text{meas}}$, while filtering the signal in the next step. Step 3: A median filter was applied to the preprocessed SpO$_2$ signal. This operation resulted in SpO$_2^{\text{clear}}$ values that reflect SaO$_2$ values without the presence of any measurement noise. Step 4: Each SpO$_2^{\text{clear}}$ datapoint was converted to an SaO$_2$ value, using an inverse function to the SaO$_2$–SpO$_2$ bias function. Each calculated SaO$_2$ value was then paired with the respective SpO$_2^{\text{meas}}$ value of the raw data waveform. Steps 3 and 4 were repeated in case of the pathological patient data to find the optimal parameter values of the median filter, as described in the next section. Step 5: The differences, SpO$_2^{\text{meas}}$ − SpO$_2^{\text{clear}}$, of all valid datapoints (i.e., all values that were not excluded in Step 1 or 2) pooled together from all patients were used for the statistical model of the SpO$_2$ measurement noise in the form of a cumulative distribution function.

Outliers larger than $\pm 6\%$ $SpO_2$ were excluded. We determined the $SpO_2$ measurement noise for two patient categories, physiological neonates and pathological neonates. Cumulative distribution functions were constructed for all $SaO_2$ values, for $SaO_2 \leq 96\%$, and for $SaO_2 \geq 97\%$.
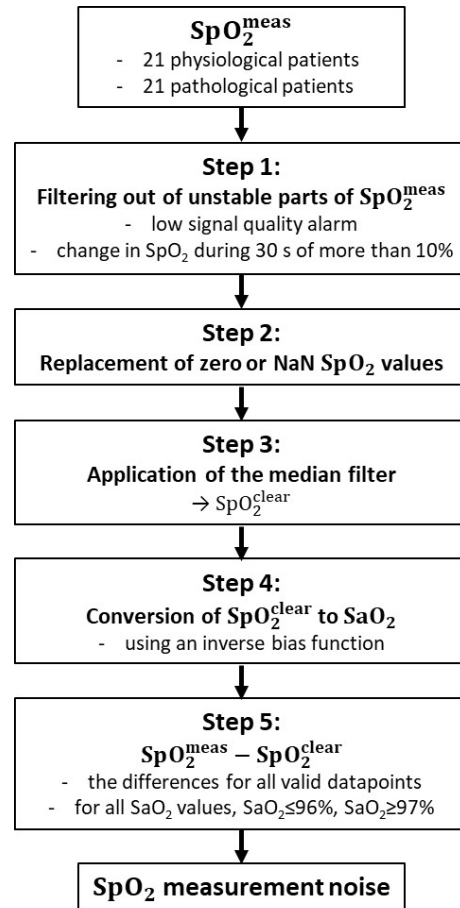
**Figure 3.** Data-processing flowchart for $SpO_2$ measurement noise estimation.
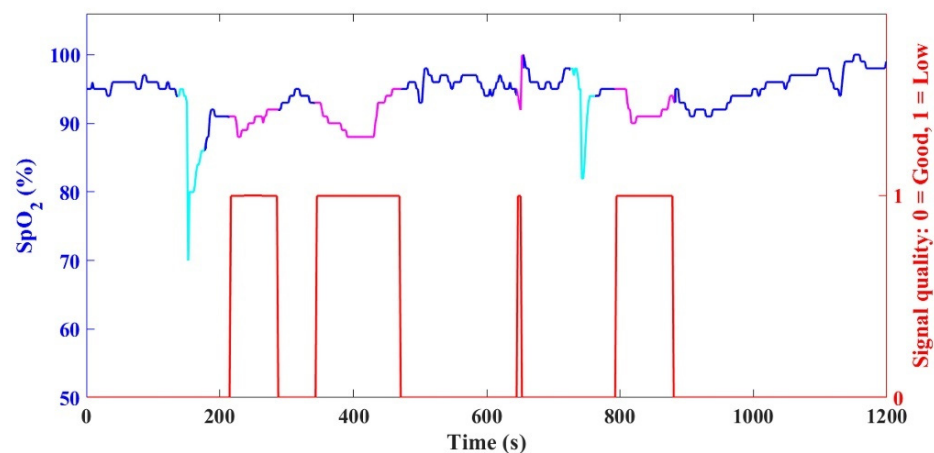
**Figure 4.** An example of the original raw $SpO_2$ data with stable parts (blue) and unstable parts (magenta and cyan). The stable parts were further processed to determine the noise, and the unstable parts were excluded due to the presence of the low-signal-quality alarm (red) or due to an abrupt change in $SpO_2$ (cyan) within a 30 s moving window.

### 2.2.2. Median Filter Window Size

At Step 3 of the SpO$_2$ measurement noise data processing, we applied the median filter to the SpO$_2$ signal to obtain noise-free SpO$_2^{clear}$ values. The optimal median filter window size was determined from the comparison of the distribution of the SpO$_2$ recordings (for each SaO$_2$ unit) from 21 pathological patients and the distribution of the data acquired by Ross et al. [11]. An assumption for comparing the two datasets was the similarity of their noise characteristics, where both datasets were of pathological patients requiring ventilatory support who were less than 60 days old. Figure 5 compares the resulting SaO$_2$–SpO$_2$ data (generated based on the outcome of Step 4) with the data of Ross et al. [11]. For each SaO$_2$ unit, a histogram of the SpO$_2$ distribution of the calculated data was compared with the respective histogram of the data of Ross et al. [11]. The filter parameters that resulted in the best overlaps of these histograms were used to construct the cumulative distribution functions in Step 5.
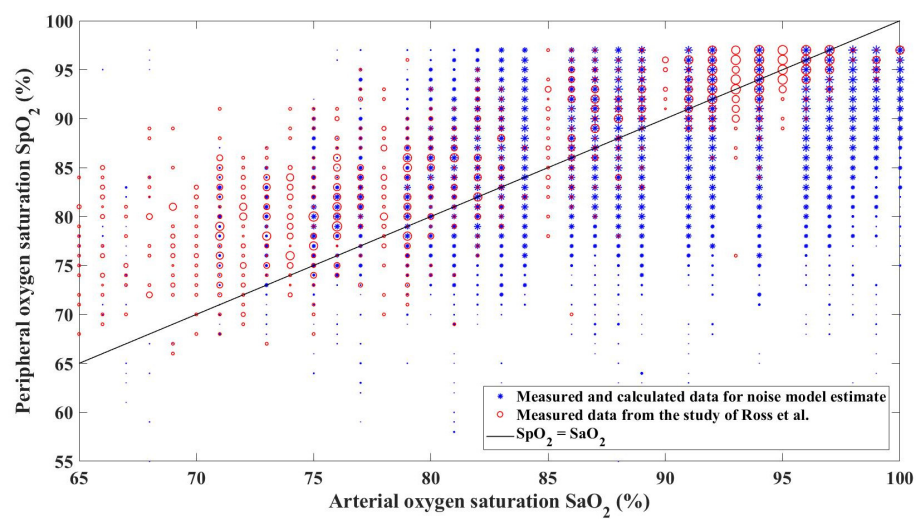
**Figure 5.** Comparison of SaO$_2$–SpO$_2$ scatterplots from the data for the noise model estimate and the data acquired by Ross et al. [11]. The diameter of a marker for each SaO$_2$–SpO$_2$ pair is proportional to the frequency of the value occurrence.

The optimal median filter window size was selected from the range 1–1000, as illustrated in Figure 6, so that it minimizes the cost function:

$$J = \frac{1}{m} \sum_{SaO_2=70}^{100} \left( 1 - \sum_{(i)} \min\left[ h_i(SpO_2^{meas}(SaO_2)), h_i\left(SpO_2^{Ross}(SaO_2)\right) \right] \right)$$

where $h_i$ is the value of an $i$-th bin of a normalized histogram of the SpO$_2$ distribution, SpO$_2^{Ross}$ refers to the data of Ross et al. [11], and $m$ is the number of SaO$_2$ units for which both the SpO$_2^{meas}$ data and SpO$_2^{Ross}$ data are available for a particular filter window size. The J function evaluates the extent to which normalized histograms of the SpO$_2$ distributions overlap at each SaO$_2$ unit and was based on the histogram intersection measure [32]. If two histograms overlap perfectly, the value of the histogram intersection measure at the particular SaO$_2$ unit is 0. On the other hand, if the histograms do not overlap at all, the value is 1. An example of partially overlapping histograms for a single window size of the median filter is presented in Figure 7. The optimal median filter window size (WDW) was set to 227 samples, which corresponds to approximately 7.5 min of pulse oximeter output samples with the sampling time of 2 s.
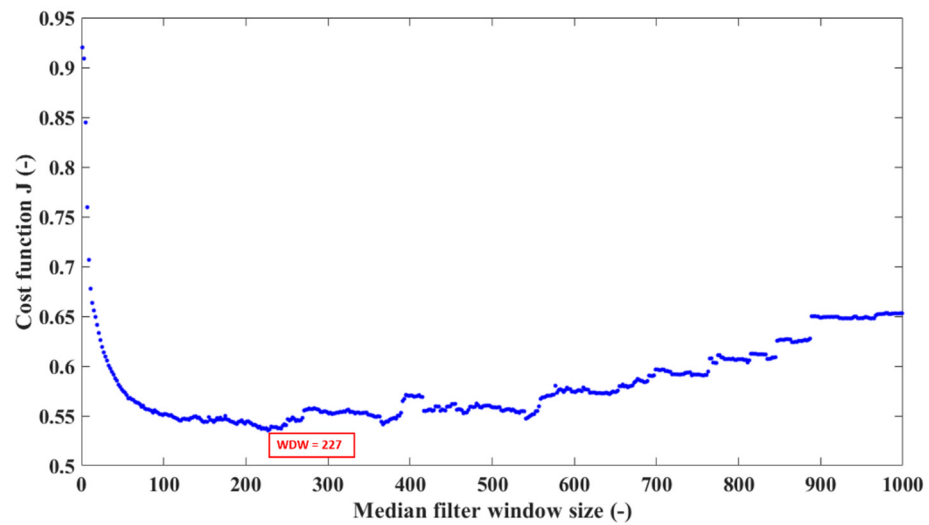
**Figure 6.** Estimating the optimal window size of the median filter by minimizing the cost function J. The optimal median filter window size (WDW) was 227 samples.
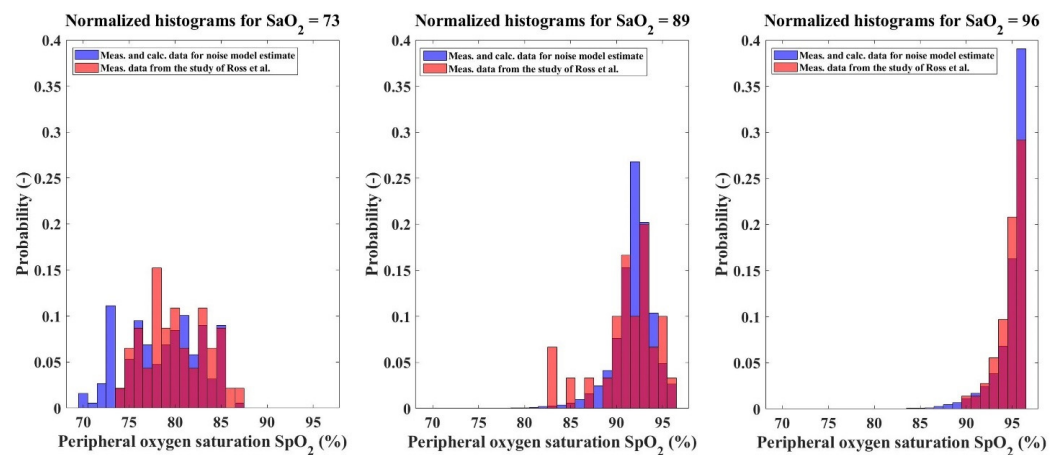
**Figure 7.** An example of partially overlapping histograms for three different $SaO_2$ units and the window size of the median filter set at 227 samples. The blue color represents the $SpO_2$ values measured to estimate the $SpO_2$ measurement noise. The red color represents the $SpO_2$ values acquired by Ross et al. [11]. The magenta color represents the histogram intersection.

### 2.2.3. Integration of $SaO_2$–$SpO_2$ Bias with $SpO_2$ Measurement Noise

The pulse oximeter model, the terminal part of a complex mathematical model of neonatal oxygenation, integrates the $SaO_2$–$SpO_2$ bias with the $SpO_2$ measurement noise. The input of the pulse oximeter model is the $SaO_2$ value. The input, sampled every 2 s, is converted to a noise-free $SpO_2$ value, using the $SaO_2$–$SpO_2$ bias function. The output of the pulse oximeter model is then obtained by adding the $SpO_2$ measurement noise generated randomly, following the probabilities specified by the cumulative distribution function to the noise-free $SpO_2$ value.

### 3. Results

The model of the output of the pulse oximeter consists of two parts: the $SaO_2$–$SpO_2$ bias and the $SpO_2$ measurement noise. The $SaO_2$–$SpO_2$ bias function was determined in our previous study [30]. The $SpO_2$ measurement noise was estimated for two different groups of patients, physiological neonates and pathological neonates. Figure 8 depicts the resulting normalized histograms of the $SpO_2$ measurement noise for both the categories for all $SaO_2$ values and also separately for $SaO_2 \leq 96\%$ and for $SaO_2 \geq 97\%$. The statistical properties of the $SpO_2$ measurement noise are expressed by the cumulative distribution

function presented in Figure 9. The exact numerical values of the cumulative distribution function are provided in Appendix A in Table A1.
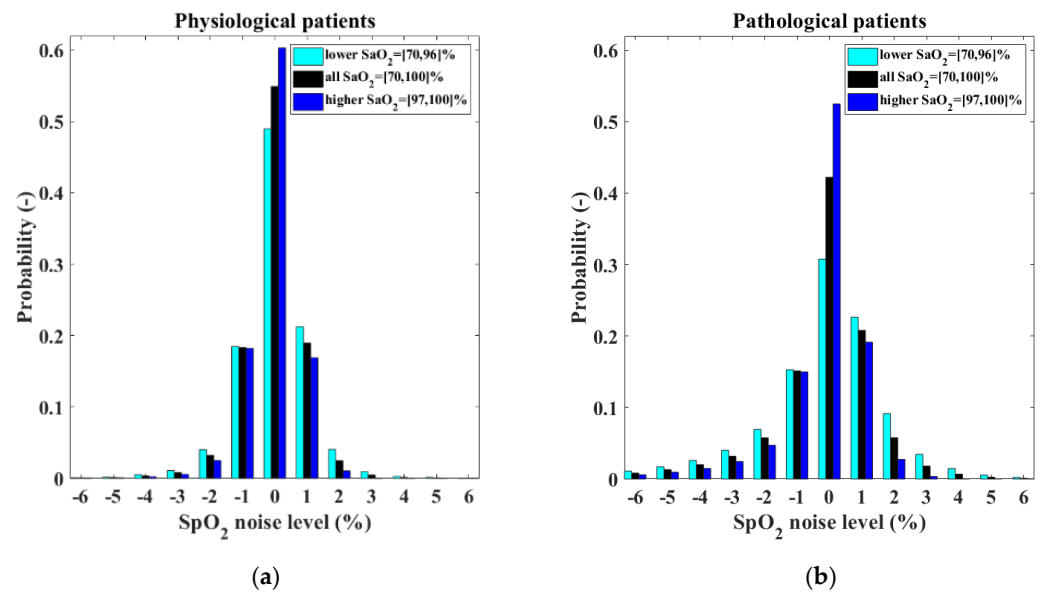
**Figure 8.** Normalized histograms of the SpO$_2$ measurement noise shows different characteristics for (**a**) physiological neonates and (**b**) pathological neonates.
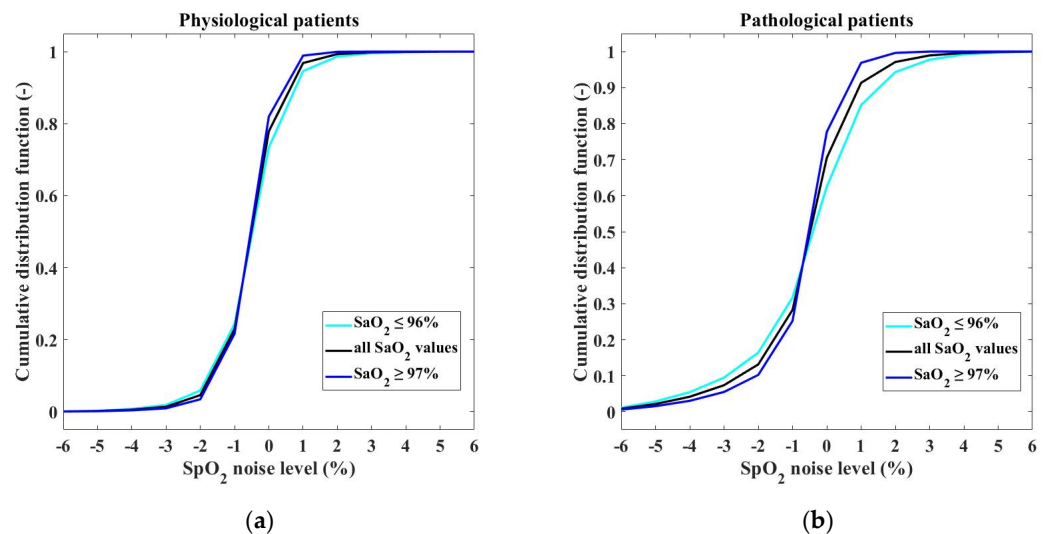
**Figure 9.** Cumulative distribution functions of the SpO$_2$ measurement noise for (**a**) physiological and (**b**) pathological patients.

In the pulse oximeter module, the random noise generated according to the characteristics presented in Figures 8 and 9 is added to the SpO$_2$ value calculated by using the SaO$_2$–SpO$_2$ bias function. Figure 10 shows the resulting SaO$_2$–SpO$_2$ scatterplot of the output of the pulse oximeter module. The figure displays the distribution of SpO$_2$ values generated for each SaO$_2$ value, including the frequency of occurrence of each SaO$_2$–SpO$_2$ pair.
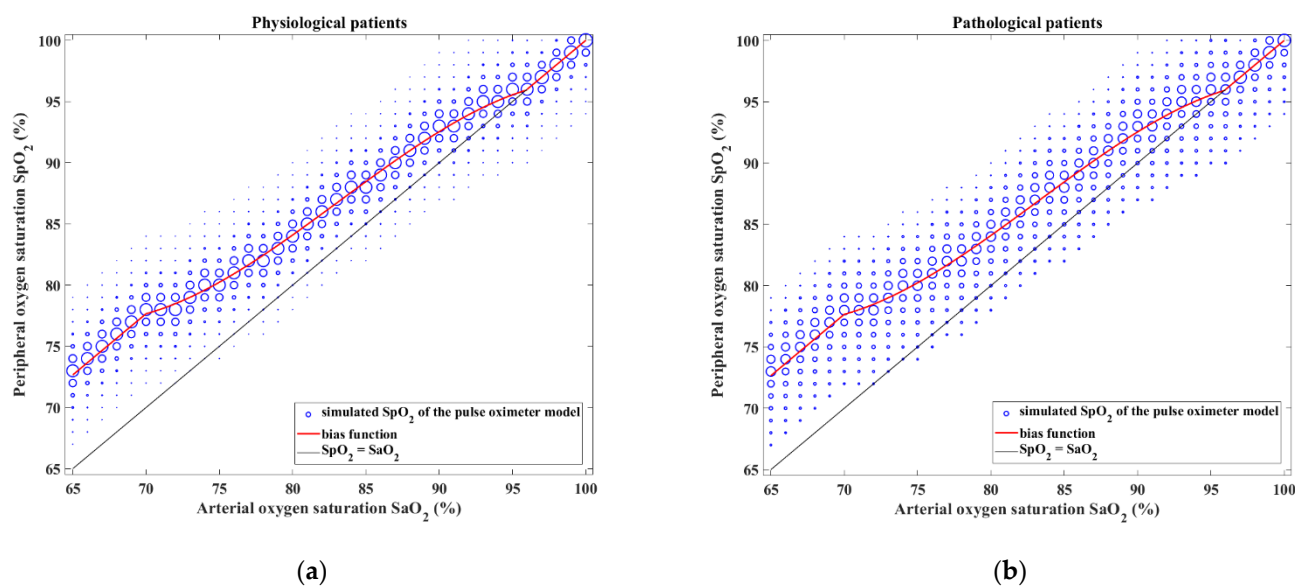
**Figure 10.** The output of the pulse oximeter model consisting of $SaO_2$–$SpO_2$ bias and $SpO_2$ measurement noise for (**a**) physiological and (**b**) pathological patients. Each $SaO_2$ value is converted to an $SpO_2$ value to which noise is added according to the properties shown in Figures 8 and 9. The size of the symbol of each $SaO_2$–$SpO_2$ pair is proportional to the frequency of its occurrence.

## 4. Discussion

In this work, we quantified the measurement noise that is characteristic for continuous $SpO_2$ time recording and completed the model of the output of the pulse oximeter typical for premature infants.

The model of the output of the pulse oximeter consists of two parts: the $SaO_2$–$SpO_2$ bias and the $SpO_2$ measurement noise. The $SaO_2$–$SpO_2$ bias was determined from the Ross' clinical data [11] in the $SaO_2$ range of 70–100% in our previous study [30]. The bias values slightly differ between previously published clinical studies [11,14,18]. This may be due to different methods of measuring $SaO_2$ (co-oximetry vs. blood gas analysis), measuring $SpO_2$, or monitoring of the patients with different age and diagnoses. However, the published differences are too small to affect the credibility of the simulated output of the pulse oximeter model and its applicability to the neonatal oxygen transport model. For $SaO_2$ values less than 70%, the bias was held constant, equal to the value of the bias for 70% $SaO_2$ (7.66%), due to the lack of clinical data. The constant bias for $SaO_2$ of less than 70% would be a sufficient approximation for the model of a neonate on oxygen support, because these values are associated with severe hypoxemia and are beyond the target range in which the saturation of ventilated premature infants should be maintained. In addition, pulse oximeter manufacturers do not guarantee the accuracy of pulse oximeter measurements of such low saturation values [33].

In addition to the interpersonal variability of $SaO_2$–$SpO_2$ bias occurring in the studies [11,13–15,18] mentioned above, intrapersonal variability due to low perfusion, motion artifacts, or another noise, such as bright light or electromagnetic interference [21,23,24], also appears in the $SpO_2$ time recordings of each patient during the bed-side monitoring. In our work, we characterized the intrapersonal variability of $SpO_2$ time recording as the $SpO_2$ measurement noise. The noise was determined for two groups, physiological neonates and pathological neonates, based on the clinical data of 21 patients in each group as the difference between the measured $SpO_2$ values and the estimated $SpO_2$ values without noise. The noise model was estimated by using a numerical procedure in which the window size of the median filter was varied. The median filter was chosen over the moving average filter because of the frequent sudden but short drops in the $SpO_2$ signal (perhaps due to moving artifacts) that we wished to remove. The advantage of the median filter is its simplicity

and ease of implementation. However, other, more sophisticated denoising methods are available, based, for example, on wavelets [34] or compressed sensing [35]. The specific filter setting determined what would be considered a noise-free $SpO_2$ signal, thus indirectly generating variations of the noise model. We considered as the most plausible the variant of the noise model that produced our $SpO_2$ data distribution the most similar to that published by Ross in his study (as expressed by the minimum of the J function). The $SpO_2$ measurement noise was described by histograms and cumulative distribution functions not only for two categories of neonates but also for two different $SaO_2$ intervals, $SaO_2 \leq 96\%$ and $SaO_2 \geq 97\%$. The boundary between the intervals was chosen to be identical to the intervals of the $SaO_2$–$SpO_2$ bias.

At the beginning of noise-signal processing, we excluded the unstable parts of the measured $SpO_2$ signal. The exclusion of all $SpO_2$ values measured during the episodes of triggered low-signal-quality alarm corresponds to automatic oxygenation control algorithms that do not consider such $SpO_2$ values reliable for automatic adjustment of the fraction of inspired oxygen [36]. In addition, all $SpO_2$ values that were the middle sample of a 30 s moving window in which $SpO_2$ changed by more than 10% were excluded. This second criterion was introduced because the distinct drops in the $SpO_2$ signal can be caused not only by artifacts but also by real desaturation, which cannot be distinguished without having the simultaneous data of the patient's movement available. Previous studies have considered motion artifacts as a major factor in inaccurate pulse oximeter readings [21,23], and this is even more influential in the group of preterm and term infants [37,38]. In comparison with adults, more motion, longer periods of motion, and more intensive motion were observed in infants [37]. Fletcher et al. [38] concluded that motion artifact can affect, overall, up to 50% of $SpO_2$ recorded time, and actually the motion artifact was present 91% of the monitored time during infant wakefulness. During the apnea, preterm infants can desaturate with a rate of 3–8% per second [39], and the study published by Poets and Southall [40] even reported the rate of up to 12.6% per second. Therefore, motion artifact and desaturation may have a similar $SpO_2$ recording, and motion artifact could be interpreted as the true desaturation and vice versa, or motion artifact can obscure the true desaturation with noise [23]. Abrupt changes in the $SpO_2$ signal due to desaturations are reflected in the pulse oximeter module, as they are generated by the overall model of neonatal oxygenation [8]. However, motion artifacts leading to significant drops in the $SpO_2$ signal (drops greater than 10% within 30 s) are not included in our model and should be modeled separately in a future study with simultaneous recording of $SpO_2$ signal and motion capture.

Our approach to the design of the pulse oximeter model can be compared with the model used by Morozoff et al. [29] in their physiological models. The main novelty of our model is that it is based on real clinical data measured on patients who are the target group for automatic control of oxygenation. The model incorporates the bias between $SaO_2$ and $SpO_2$, the presence of which is documented by many studies [11–19]. Furthermore, it proposes different noise levels according to the stability of the patients (physiological or pathological) and according to the input $SaO_2$ value, since, as the histograms in Figure 8 show, the noise distribution for low and high $SaO_2$ values is different.

The main limitations of the pulse oximeter model are the datasets used to determine the $SaO_2$–$SpO_2$ bias and $SpO_2$ measurement noise. One general $SaO_2$–$SpO_2$ bias function was based on the multicenter study on a relatively large number of patients from different PICUs, but the biases among children may systematically vary depending on its diagnosis [11,20], amount of fetal hemoglobin [11,14,20,22], or skin pigmentation [21,23]. The bias may also vary between different $SpO_2$ monitors or sensors [24], or between different sensor placements [15,20,21]. The noise model was determined based on comprehensive data from both physiological and pathological neonates; moreover, the amount of measured data allowed for the determination of noise characteristics for different $SaO_2$ intervals. The noise was estimated from the data measured at one setting of the pulse oximeter averaging time. The averaging time is usually adjustable in a range between 2 and 16 s and can significantly

affect the stability of pulse oximeter readings [33] and resulting noise characteristics. We determined the noise characteristic only for 8 s averaging (with an output update every 2 s), but it might be interesting to compare the noise characteristic of different averaging time settings. Moreover, the median filter we used for the noise estimation, as discussed above, may be disputed. Finally, due to the exclusion of the unstable parts of $SpO_2$ signal, our model of the $SaO_2$–$SpO_2$ relationship does not describe the effect of some motion artifacts that trigger the low-signal-quality alarm, as discussed in the previous paragraph.

The results of the work will improve the pulse oximeter model, which is the terminal part of the neonatal oxygen transport model, so that the simulated output of the model, the peripheral oxygen saturation, will more realistically represent the real $SpO_2$ signals observed in the clinical environment. This work and further improvements of the complex mathematical model will enhance the in silico testing and comparison of existing and future control algorithms under real clinical conditions. There is a need for improved modeling that reflects the dynamics of the neonatal oxygen transport system to achieve optimal control across the full spectrum of oxygenation disturbances, including the possibility of individualization of algorithm performance [10].

## 5. Conclusions

This work proposed methods for determining the measurement noise characteristics in peripheral oxygen saturation signal in combination with the bias between $SaO_2$ and $SpO_2$. The terminal part of the neonatal oxygen transport model, the pulse oximeter module, was improved in two ways: we determined the characteristics of the noise presented in $SpO_2$ time-recordings during the premature infant bedside monitoring, and we combined the $SpO_2$ measurement noise with $SaO_2$–$SpO_2$ bias. These results will improve the output of the neonatal oxygenation model and make simulations provided by the computer model of oxygenation of a neonate closer to the real situations observed in the clinical practice.

**Author Contributions:** V.R.-H., J.R., K.M. and T.E.B. conceptualized the research; T.E.B. and P.K. acquired the data; all authors contributed to the methodology of data analysis; V.R.-H. and J.R. performed data analysis, interpretation, and visualization; V.R.-H. and J.R. drafted the manuscript; K.M. and M.R. supervised the research. All authors reviewed and revised the manuscript. All authors have read and agreed to the published version of the manuscript.

**Funding:** The work was supported by grants SGS20/202/OHK4/3T/17, SGS22/202/OHK4/3T/17, and SGS22/204/OHK4/3T/17 of Czech Technical University in Prague.

**Data Availability Statement:** The dataset used and analyzed for the noise model estimate is available from the corresponding author upon reasonable request.

**Acknowledgments:** The authors thank Patrick A. Ross et al. and General University Hospital in Prague for providing clinical data.

**Conflicts of Interest:** The authors declare no conflict of interest.

## Appendix A

**Table A1.** Cumulative distribution function of the $SpO_2$ measurement noise.

| SpO$_2$ Noise Level (%) | CDF for Physiological Patients (–) | | | CDF for Pathological Patients (–) | | |
|---|---|---|---|---|---|---|
| | All SaO$_2$ Values | SaO$_2 \leq 96\%$ | SaO$_2 \geq 97\%$ | All SaO$_2$ Values | SaO$_2 \leq 96\%$ | SaO$_2 \geq 97\%$ |
| −6 | 0.0007 | 0.0009 | 0.0006 | 0.0085 | 0.0112 | 0.0060 |
| −5 | 0.0020 | 0.0025 | 0.0015 | 0.0217 | 0.0284 | 0.0157 |
| −4 | 0.0056 | 0.0076 | 0.0039 | 0.0418 | 0.0544 | 0.0305 |
| −3 | 0.0138 | 0.0186 | 0.0095 | 0.0738 | 0.0947 | 0.0551 |
| −2 | 0.0461 | 0.0589 | 0.0346 | 0.1316 | 0.1642 | 0.1025 |
| −1 | 0.2295 | 0.2436 | 0.2167 | 0.2830 | 0.3171 | 0.2524 |
| 0 | 0.7786 | 0.7333 | 0.8198 | 0.7052 | 0.6247 | 0.7773 |
| 1 | 0.9683 | 0.9457 | 0.9889 | 0.9132 | 0.8512 | 0.9688 |
| 2 | 0.9932 | 0.9863 | 0.9995 | 0.9711 | 0.9429 | 0.9964 |

**Table A1.** *Cont.*

| SpO$_2$ Noise Level (%) | CDF for Physiological Patients (–) | | | CDF for Pathological Patients (–) | | |
|---|---|---|---|---|---|---|
| | **All SaO$_2$ Values** | **SaO$_2$ ≤ 96%** | **SaO$_2$ ≥ 97%** | **All SaO$_2$ Values** | **SaO$_2$ ≤ 96%** | **SaO$_2$ ≥ 97%** |
| 3 | 0.9980 | 0.9957 | 1.0000 | 0.9893 | 0.9774 | 1.0000 |
| 4 | 0.9992 | 0.9984 | – | 0.9962 | 0.9920 | – |
| 5 | 0.9998 | 0.9997 | – | 0.9989 | 0.9977 | – |
| 6 | 1.0000 | 1.0000 | – | 1.0000 | 1.0000 | – |

## References

1. Fathabadi, O.S.; Gale, T.J.; Olivier, J.C.; Dargaville, P.A. Automated control of inspired oxygen for preterm infants: What we have and what we need. *Biomed. Signal Process. Control* **2016**, *28*, 9–18. [CrossRef]
2. Claure, N.; Bancalari, E. Closed-loop control of inspired oxygen in premature infants. *Semin. Fetal Neonatal Med.* **2015**, *20*, 198–204. [CrossRef] [PubMed]
3. Sanchez-Morillo, D.; Olaby, O.; Fernandez-Granero, M.A.; Leon-Jimenez, A. Physiological closed-loop control in intelligent oxygen therapy: A review. *Comput. Methods Programs Biomed.* **2017**, *146*, 101–108. [CrossRef] [PubMed]
4. Mitra, S.; Singh, B.; El-Naggar, W.; McMillan, D.D. Automated versus manual control of inspired oxygen to target oxygen saturation in preterm infants: A systematic review and meta-analysis. *J. Perinatol.* **2018**, *38*, 351–360. [CrossRef]
5. Sturrock, S.; Williams, E.; Dassios, T.; Greenough, A. Closed loop automated oxygen control in neonates—A review. *Acta Paediatr.* **2019**, *109*, 914–922. [CrossRef]
6. Dani, C. Automated control of inspired oxygen (FiO$_2$) in preterm infants: Literature review. *Pediatr. Pulmonol.* **2019**, *54*, 358–363. [CrossRef]
7. Morozoff, E.P.; Saif, M. Oxygen therapy control of neonates—Part I: A model of neonatal oxygen transport. *Control Intell. Syst.* **2008**, *36*, 227–237. [CrossRef]
8. Rafl, J.; Bachman, T.E.; Martinek, T.; Tejkl, L.; Huttova, V.; Kudrna, P.; Roubik, K. Design and Demonstration of a Complex Neonatal Physiological Model for Testing of Novel Closed-Loop Inspired Oxygen Fraction Controllers. In *World Congress on Medical Physics and Biomedical Engineering 2018, Proceedings of the IUPESM World Congress on Medical Physics and Biomedical Engineering, Prague, Czech Republic, 3–8 June 2018*; Lhotska, L., Sukupova, L., Lacković, I., Ibbott, G., Eds.; Springer: Singapore, 2019; pp. 725–729. [CrossRef]
9. Rafl, J.; Huttova, V.; Möller, K.; Bachman, T.E.; Tejkl, L.; Kudrna, P.; Rozanek, M.; Roubik, K. Computer model of oxygenation in neonates. *Curr. Dir. Biomed. Eng.* **2019**, *5*, 73–76. [CrossRef]
10. Dargaville, P.A.; Marshall, A.P.; McLeod, L.; Salverda, H.H.; te Pas, A.B.; Gale, T.J. Automation of oxygen titration in preterm infants: Current evidence and future challenges. *Early Hum. Dev.* **2021**, *162*, 105462. [CrossRef]
11. Ross, P.A.; Newth, C.J.L.; Khemani, R.G. Accuracy of Pulse Oximetry in Children. *Pediatrics* **2014**, *133*, 22–29. [CrossRef]
12. Bohnhorst, B.; Peter, C.S.; Poets, C.F. Detection of hyperoxaemia in neonates: Data from three new pulse oximeters. *Arch. Dis. Child Fetal Neonatal Ed.* **2002**, *87*, F217–F219. [CrossRef] [PubMed]
13. Gerstmann, D.; Berg, R.; Haskell, R.; Brower, C.; Wood, K.; Yoder, B.; Greenway, L.; Lassen, G.; Ogden, R.; Stoddard, R.; et al. Operational Evaluation of Pulse Oximetry in NICU Patients with Arterial Access. *J. Perinatol.* **2003**, *23*, 378–383. [CrossRef] [PubMed]
14. Rosychuk, R.J.; Hudson-Mason, A.; Eklund, D.; Lacaze-Masmonteil, T. Discrepancies between Arterial Oxygen Saturation and Functional Oxygen Saturation Measured with Pulse Oximetry in Very Preterm Infants. *Neonatology* **2012**, *101*, 14–19. [CrossRef] [PubMed]
15. Harris, B.U.; Char, D.S.; Feinstein, J.A.; Verma, A.; Shiboski, S.C.; Ramamoorthy, C. Accuracy of Pulse Oximeters Intended for Hypoxemic Pediatric Patients. *Pediatr. Crit. Care Med.* **2016**, *17*, 315–320. [CrossRef] [PubMed]
16. Harris, B.U.; Stewart, S.; Verma, A.; Hoen, H.; Stein, M.L.; Wright, G.; Ramamoorthy, C. Accuracy of a portable pulse oximeter in monitoring hypoxemic infants with cyanotic heart disease. *Cardiol. Young* **2019**, *29*, 1025–1029. [CrossRef] [PubMed]
17. Murphy, D.; Pak, Y.; Cleary, J.P. Pulse Oximetry Overestimates Oxyhemoglobin in Neonates with Critical Congenital Heart Disease. *Neonatology* **2016**, *109*, 213–218. [CrossRef]
18. Bachman, T.E.; Newth, C.J.L.; Ross, P.A.; Iyer, N.P.; Khemani, R.G. Characterization of the bias between oxygen saturation measured by pulse oximetry and calculated by an arterial blood gas analyzer in critically ill neonates. *Lek. Technol.* **2017**, *47*, 130–134.
19. Griksaitis, M.J.; Scrimgeour, G.E.; Pappachan, J.V.; Baldock, A.J. Accuracy of the Masimo SET® LNCS neo peripheral pulse oximeter in cyanotic congenital heart disease. *Cardiol. Young* **2016**, *26*, 1183–1186. [CrossRef]
20. Lakshminrusimha, S.; Manja, V.; Mathew, B.; Suresh, G.K. Oxygen targeting in preterm infants: A physiological interpretation. *J. Perinatol.* **2015**, *35*, 8–15. [CrossRef]
21. Jubran, A. Pulse oximetry. *Crit. Care* **2015**, *19*, 272. [CrossRef]
22. Shiao, S.Y. Effects of fetal hemoglobin on accurate measurements of oxygen saturation in neonates. *J. Perinat. Neonatal Nurs.* **2005**, *19*, 348–361. [CrossRef] [PubMed]

23. Petterson, M.T.; Begnoche, V.L.; Graybeal, J.M. The Effect of Motion on Pulse Oximetry and Its Clinical Significance. *Anesth. Analg.* **2007**, *105*, S78–S84. [CrossRef] [PubMed]

24. Sola, A.; Golombek, S.G.; Montes Bueno, M.T.; Lemus-Varela, L.; Zuluaga, C.; Domínguez, F.; Baquero, H.; Young Sarmiento, A.E.; Natta, D.; Rodriguez Perez, J.M.; et al. Safe oxygen saturation targeting and monitoring in preterm infants: Can we avoid hypoxia and hyperoxia? *Acta Paediatr.* **2014**, *103*, 1009–1018. [CrossRef]

25. Fine, J.; Branan, K.L.; Rodriguez, A.J.; Boonya-Ananta, T.; Ramella-Roman, J.C.; McShane, M.J.; Coté, G.L.. Sources of Inaccuracy in Photoplethysmography for Continuous Cardiovascular Monitoring. *Biosensors* **2021**, *11*, 126. [CrossRef] [PubMed]

26. Lee, J.; Kim, M.; Park, H.-K.; Kim, I.Y. Motion Artifact Reduction in Wearable Photoplethysmography Based on Multi-Channel Sensors with Multiple Wavelengths. *Sensors* **2020**, *20*, 1493. [CrossRef] [PubMed]

27. Sabeti, E.; Reamaroon, N.; Mathis, M.; Gryak, J.; Sjoding, M.; Najarian, K. Signal quality measure for pulsatile physiological signals using morphological features: Applications in reliability measure for pulse oximetry. *Inform. Med. Unlocked* **2019**, *16*, 100222. [CrossRef] [PubMed]

28. Pereira, T.; Gadhoumi, K.; Ma, M.; Liu, X.; Xiao, R.; Colorado, R.A.; Keenan, K.J.; Meisel, K.; Hu, X. A Supervised Approach to Robust Photoplethysmography Quality Assessment. *IEEE J. Biomed. Health Inform.* **2020**, *24*, 649–657. [CrossRef]

29. Morozoff, E.P.; Smyth, J.A.; Saif, M. Applying Computer Models to Realize Closed-Loop Neonatal Oxygen Therapy. *Anesth. Analg.* **2017**, *124*, 95–103. [CrossRef]

30. Huttova, V.; Rafl, J.; Möller, K.; Bachman, T.E.; Kudrna, P.; Rozanek, M.; Roubik, K. Model of SpO2 signal of the neonate. *Curr. Dir. Biomed. Eng.* **2019**, *5*, 549–552. [CrossRef]

31. Wellington, G.; Elder, D.; Campbell, A. 24-hour oxygen saturation recordings in preterm infants: Editing artefact. *Acta Paediatr.* **2018**, *107*, 1362–1369. [CrossRef]

32. Cha, S.-H.; Srihari, S.N. On measuring the distance between histograms. *Pattern Recognit.* **2002**, *35*, 1355–1370. [CrossRef]

33. Rad-97™ Pulse CO-Oximeter—Operator's Manual. Available online: https://techdocs.masimo.com/globalassets/techdocs/pdf/lab-9275d_master.pdf (accessed on 23 February 2022).

34. Ouahabi, A. (Ed.) *Signal and Image Multiresolution Analysis*; ISTE-Wiley: London, UK; Hoboken, NJ, USA, 2013.

35. Haneche, H.; Boudraa, B.; Ouahabi, A. A new way to enhance speech signal based on compressed sensing. *Measurement* **2020**, *151*, 107117. [CrossRef]

36. Hallenberger, A.; Poets, C.F.; Horn, W.; Seyfang, A.; Urschitz, M.S. Closed-Loop Automatic Oxygen Control (CLAC) in Preterm Infants: A Randomized Controlled Trial. *Pediatrics* **2014**, *133*, e379–e385. [CrossRef] [PubMed]

37. Tobin, R.M.; Pologe, J.A.; Batchelder, P.B. A Characterization of Motion Affecting Pulse Oximetry in 350 Patients. *Anesth. Analg.* **2002**, *94*, S54–S61. [PubMed]

38. Fletcher, J.; Page, M.; Jeffery, H.E. Sleep States and Neonatal Pulse Oximetry. *Sleep* **1998**, *21*, 305–310. [CrossRef] [PubMed]

39. Sands, S.A.; Edwards, B.A.; Kelly, V.J.; Davidson, M.R.; Wilkinson, M.H.; Berger, P.J. A Model Analysis of Arterial Oxygen Desaturation during Apnea in Preterm Infants. *PLoS Comput. Biol.* **2009**, *5*, e1000588. [CrossRef]

40. Poets, C.F.; Southall, D.P. Patterns of oxygenation during periodic breathing in preterm infants. *Early Hum. Dev.* **1991**, *26*, 1–12. [CrossRef]